Pamukkale Üniversitesi Mühendislik Bilimleri Dergisi
Pamukkale University Journal of Engineering Sciences

Synthesis, characterization, and photocatalytic performance evaluation of manganese tungstate for methyl red dye degradation

Mangan Tungstat'ın Sentezi, karakterizasyonu ve metil kırmızı boya giderimi için fotokatalitik performans değerlendirmesi

Mehmet KAYHAN[1], Emine KAYHAN[2]*

[1]Scientific Analysis Technological Application and Research Center, Usak University, Usak University, Uşak, Türkiye.
mehmet.kayhan@usak.edu.tr
[2]Department of Quality Coordinatorship, Usak University, Uşak University, Uşak, Türkiye.
emine.kayhan@usak.edu.tr

Received/Geliş Tarihi: 17.01.2025 Revision/Düzeltme Tarihi: 13.03.2025 doi: 10.5505/pajes.2025.27723
Accepted/Kabul Tarihi: 19.03.2025 Research Article/Araştırma Makalesi

Abstract

The increasing prevalence of synthetic dyes in industrial wastewater presents significant environmental challenges because of the toxicity and lack of effectiveness of conventional treatment methods. Methyl red, a widely used azo dye, is particularly problematic due to its high chemical stability. In this study, manganese tungstate ($MnWO_4$) was synthesized using a coprecipitation method and evaluated for its photocatalytic activity in methyl red degradation through UV-C exposure. The synthesized $MnWO_4$ was characterized using several techniques, including Fourier transform infrared spectroscopy (FTIR), ultraviolet-diffuse reflectance spectroscopy (UV-DRS), and scanning electron microscopy (SEM). SEM analysis revealed the formation of needle-like, nanometer-sized $MnWO_4$ particles with high aspect ratios, which are expected to enhance photocatalytic efficiency. XRD confirmed the development of a highly crystalline pure $MnWO_4$ phase, and FTIR spectra showed characteristic peaks corresponding to Mn–O and W–O bonds. The UV-DRS results revealed that the material possesses a direct band gap of 3.18 eV, suitable for UV-C light absorption. Photocatalytic experiments demonstrated that $MnWO_4$ effectively degraded methyl red, with the removal efficiency reaching nearly 60% after 180 minutes of irradiation. These findings suggest that $MnWO_4$ is a promising photocatalyst for environmental remediation, offering a simple, cost-effective solution for dye degradation in wastewater.

Keywords: Manganese tungstate ($MnWO_4$), Photocatalysis, Methyl red degradation, Wastewater treatment, Dye degradation, Environmental remediation

Öz

Sentezlenen sentetik boyaların sanayi atıksularındaki artan yaygınlığı, toksisiteleri ve geleneksel arıtma yöntemlerine karşı dirençleri nedeniyle önemli çevresel zorluklar yaratmaktadır. Yaygın olarak kullanılan bir azo boyası olan metil kırmızı, yüksek kimyasal kararlılığı nedeniyle özellikle sorun teşkil eder. Bu çalışmada, manganez tungstat ($MnWO_4$), ko-precipitasyon yöntemi kullanılarak sentezlenmiş ve UV-C ışınımı altında metil kırmızının fotokatalitik bozunumu için değerlendirilmiştir. Sentezlenen $MnWO_4$, X-ışını kırınımı (XRD), Fourier dönüşüm infrared spektroskopisi (FTIR), Ultraviyole-difüz reflektans spektroskopisi (UV-DRS) ve Taramalı elektron mikroskobu (SEM) gibi çeşitli tekniklerle karakterize edilmiştir. SEM analizi, yüksek açısal oranlara sahip iğne benzeri, nanometre boyutlarında $MnWO_4$ parçacıklarının oluşumunu ortaya koymuştur, bu da fotokatalitik verimliliği artırması beklenen bir özelliktir. XRD, yüksek kristal yapıda saf bir $MnWO_4$ fazının oluşumunu doğrulamış ve FTIR spektrumları, Mn–O ve W–O bağlarına karşılık gelen karakteristik pikleri göstermiştir. UV-DRS sonuçları, malzemenin UV-C ışığı emme için uygun olan 3.18 eV'lik bir direk bant aralığına sahip olduğunu göstermektedir. Fotokatalitik deneyler, $MnWO_4$'ün metil kırmızıyı etkin bir şekilde bozduğunu ve 180 dakika sonra bozunma verimliliğinin neredeyse %60'a ulaştığını göstermiştir. Bu bulgular, $MnWO_4$'ün çevresel iyileştirme için umut verici bir fotokatalizör olduğunu ve atıksulardaki boya bozulması için basit ve maliyet etkin bir çözüm sunduğunu göstermektedir.

Anahtar kelimeler: Mangan tungstat ($MnWO_4$), fotokataliz, metil kırmızı bozunumu, atıksu arıtımı, boya bozunumu, çevresel iyileştirme

1 Introduction

The growing prevalence of synthetic dyes in manufacturing-related wastewater poses significant environmental challenges because of their harmful nature and resistance to biodegradation, and potential to accumulate in aquatic ecosystems [1]-[7]. Among these dyes, methyl red, a widely used azo dye, is particularly problematic owing to its strong chemical stability and inability to undergo degradation conventional wastewater treatment methods [8]-[10]. The release of such pollutants into water bodies not only disrupts ecosystems but also threatens human health, highlighting the urgent need for effective remediation strategies [11]-[13].

Advanced oxidation processes (AOPs) have been recognized as an effective approach for breaking down persistent organic contaminants. [14], [15]. Among these, photocatalysis has gained significant attention due to its ability to utilize solar energy to generate reactive oxygen species, responsible for decomposing complex organic species into simpler, less harmful byproducts [16], [17]. The effectiveness of a photocatalytic process is largely determined by the characteristics of the photocatalyst employed, including its bandgap, stability, and surface characteristics [18], [19].

Transition-metal tungstates, including materials such as Bi_2WO_6, $ZnWO_4$, and $CaWO_4$, have shown remarkable potential in photocatalytic applications due to their narrow bandgap, excellent thermal stability, and robust electronic properties [6],

*Corresponding author/Yazışılan Yazar

[20]-[22]. For example, Bi_2WO_6 has been widely researched for its superior photocatalytic performance when exposed to visible light, making it a benchmark material in this field [23], [24]. Similarly, $ZnWO_4$ has been recognized for its ability to degrade various organic pollutants under UV light [25], [26]. Despite these advancements, manganese tungstate ($MnWO_4$), a member of the same family of tungstates, remains underexplored.

$MnWO_4$ exhibits unique electronic and structural properties that make it a promising candidate for photocatalytic applications [27], [28]. Its narrow bandgap enables effective utilization of visible light, while its robust crystalline structure ensures stability under operational conditions [29], [30]. Recent studies have highlighted the potential of manganese-based oxides in environmental remediation, suggesting that $MnWO_4$ could exhibit excellent photocatalytic properties [31]-[33]. However, comprehensive investigations into its synthesis, characterization, and application for dye degradation, specifically for azo dyes like methyl red, are still lacking.

This study aims to address this gap by synthesizing $MnWO_4$ using a coprecipitation method and characterizing its morphological, structural, and optical characteristics through various techniques. The synthesized material's photocatalytic activity is evaluated for methyl red degradation upon exposure to visible light, providing insights into its effectiveness as an environmentally friendly catalyst.

The outcomes of this research are expected to contribute to the growing body of knowledge on transition-metal tungstates and their application in environmental remediation. By investigating the capacity of$MnWO_4$ in degradating methyl red, this study not only highlights its practical applicability but also lays the foundation for future research on manganese-based photocatalysts in addressing environmental pollution.

2 Materials and methos

Materials

The chemicals used in the synthesis, including sodium tungstate dihydrate ($Na_2WO_4{\cdot}2H_2O$) and manganese chloride tetrahydrate ($MnCl_2{\cdot}4H_2O$), had analytical grade quality and were purchased from Thermo Scientific. These chemicals were used as received, without any additional purification.

Synthesis of Manganese Tungstate

To synthesize manganese tungstate, 6 mmol of sodium tungstate dihydrate and 6 mmol of manganese chloride tetrahydrate were individually dissolved in 50 mL of ultra-pure water. Manganese chloride solution was gradually added drop by drop to the sodium tungstate solution with constant stirring. During the addition, the formation of a precipitate was observed.

After the addition was complete, stirring was continued for an additional 1 hour to ensure thorough mixing. The obtained precipitate was separated by filtration and repeatedly washed with distilled water to eliminate impurities. The filtered product was heat treated at 600°C for 5 hours. Finally, the calcined material was ground into a fine powder using an agate mortar, yielding the manganese tungstate product.

Characterization

The $MnWO_4$ sample synthesized via the coprecipitation method was subjected to various characterization techniques to analyze its properties. Phase analysis was carried out using a Rigaku Miniflex X-ray diffractometer with Cu Kα radiation. XRD patterns were recorded over a 2θ range of 10° to 90°. FTIR spectrum was collected using an ATR attachment (Spectrum Two, Perkin Elmer) in the wavenumber range of 400–4000 cm^{-1}. UV-DRS measurements were conducted to determine the band gap energy of the sample. The sample's morphology was analyzed using a Phenom ProX SEM fitted with a CeB_6 electron gun.

Photocatalytic Behavior Evaluation of Manganese Tungstate

Photocatalytic experiments were conducted using a custom-designed photocatalysis system equipped with six UV-C lamps arranged in a circular pattern around a quartz cylindrical reactor. The solution in the reactor was continuously stirred using a magnetic stirrer, while air was bubbled through the system to ensure homogeneity and oxygenation. To prevent overheating caused by UV-C exposure, the reactor's outer chamber was cooled with air.

Methyl Red (MR) dye was prepared at a concentration of 400 ppm in an ethanol-distilled water mixture with a 40:60 ratio. From this stock solution, a 10 ppm MR solution was prepared by diluting it with distilled water to a total volume of 500 mL. The solution's pH was modified to 1.5 with the addition of HCl. For the photocatalytic experiments, 200 mg of manganese tungstate catalyst was added to the MR solution. The mixture was agitated and aerated in the reactor for 30 minutes to achieve adsorption equilibrium before initiating UV-C irradiation.

The photocatalytic activity of the manganese tungstate was assessed by a Perkin Elmer Lambda 35 UV-Vis Spectrophotometer. Absorbance measurements were taken initially at 0 minutes, immediately after the adsorption equilibrium was reached. Subsequently, the system was exposed to UV-C light, and UV-Vis measurements were taken at 15-minute intervals over a total irradiation time of 180 minutes. The absorbance was recorded across the wavelength range of 300–650 nm to monitor the degradation of MR dye.

3 Results and discussion

Figure 1 displays SEM images of the synthesized $MnWO_4$ samples, at 5000X magnification (Figure 1A) and 15000X magnification (Figure 1B). The SEM images clearly reveal needle-like, nanometer-sized $MnWO_4$ particles. This morphological structure can be attributed to the anisotropic growth process, where growth occurs more rapidly along one axis than along the others during the coprecipitation synthesis of $MnWO_4$. The needle-like morphology of $MnWO_4$ offers a high aspect ratio, which is expected to enhance its photocatalytic performance.

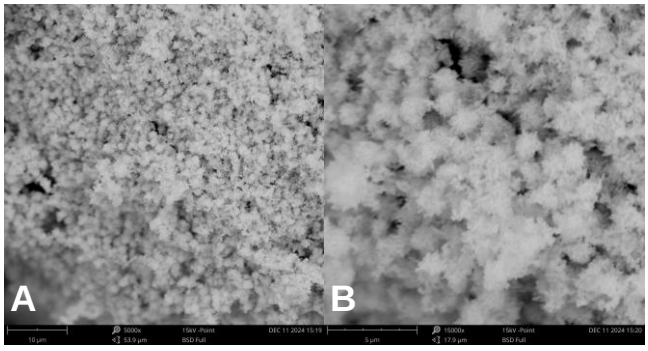

Figure 1. SEM images of synthesized MnWO4 samples A-5000X and B-15000X magnification.

The $MnWO_4$ was effectively produced through a straightforward coprecipitation method, and subsequently subjected to heat treatment in an open atmosphere. XRD confirmed the development of a highly crystalline pure $MnWO_4$ phase. As shown in Figure 2, the XRD pattern aligns well with the reference data from JCPDS Card No. 01-080-0152, with all observed peaks corresponding to the $MnWO_4$ phase. The sharp and distinct peaks in the pattern indicate that the synthesized sample possesses high crystallinity.

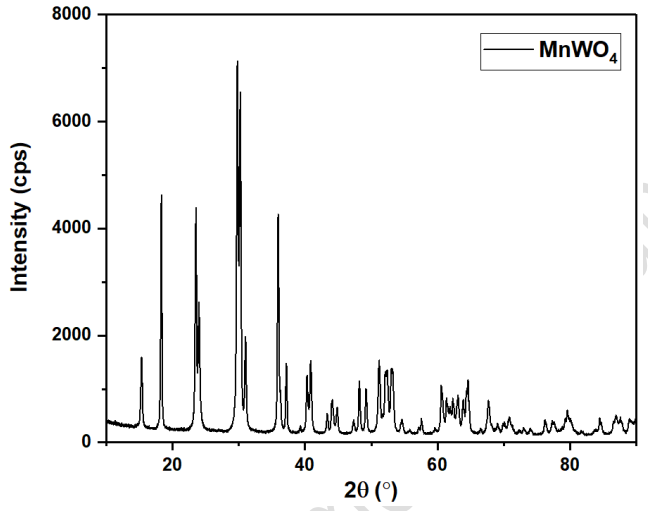

Figure 2. XRD pattern of the synthesized manganese tungstate sample, confirming its phase purity and good crystallinity. The diffraction peaks correspond closely with those of the standard JCPDS Card No. 01-080-0152, indicating the successful formation of the $MnWO_4$ phase.

The FTIR spectrum of the synthesized $MnWO_4$ was shown in Figure 3. The absorption peaks at 880 cm^{-1} and 793 cm^{-1} correspond to the symmetric and asymmetric stretching vibration modes of the W–O bond in the WO_2 terminal group, respectively [34]. The peak observed at 727 cm^{-1} is attributed to the asymmetric stretching vibrations of the W–O bond in the (W_2O_4) structural network. Peaks at 579 cm^{-1} and 558 cm^{-1} are assigned to the stretching vibrations of the Mn–O bond [35], [36].

Additionally, a weak band at 521 cm^{-1} is ascribed to the stretching vibrations of the Mn–O–Mn bond, while the low-intensity peak at 455 cm^{-1} corresponds to the in-plane deformation modes of the longest W–O bond. Lastly, the peak at 425 cm^{-1} is attributed to the in-plane deformation vibration mode of the W–O bond in the WO_2 terminal groups [36].

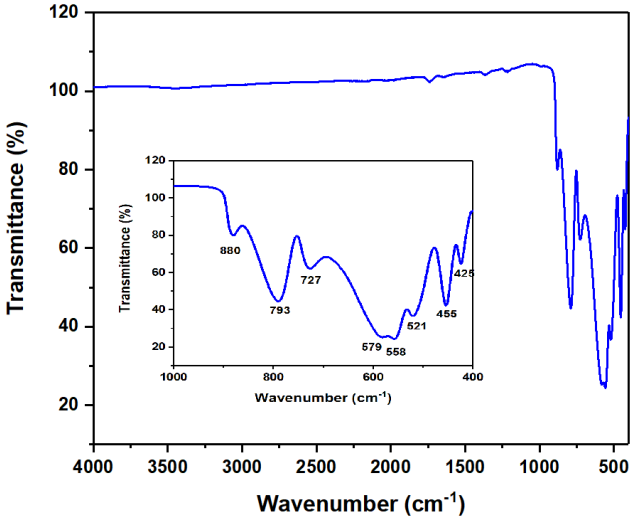

Figure 3. FTIR spectrum of the synthesized $MnWO_4$. Inset shows the bands in the range of 400-1000cm^{-1}

The light absorption characteristics $MnWO_4$ sample were examined using UV-DRS (see Figure 4). A prominent reflection peak at 518 nm was observed, which is attributed to the electronic transition between the O-2p and Mn-3d levels in $MnWO_4$. Additionally, a weaker band at 563 nm corresponds to the spin-forbidden transition between the e_g and t_{2g} orbitals of Mn-2p [37]. These findings align with those reported by Van Hanh et al. [38].

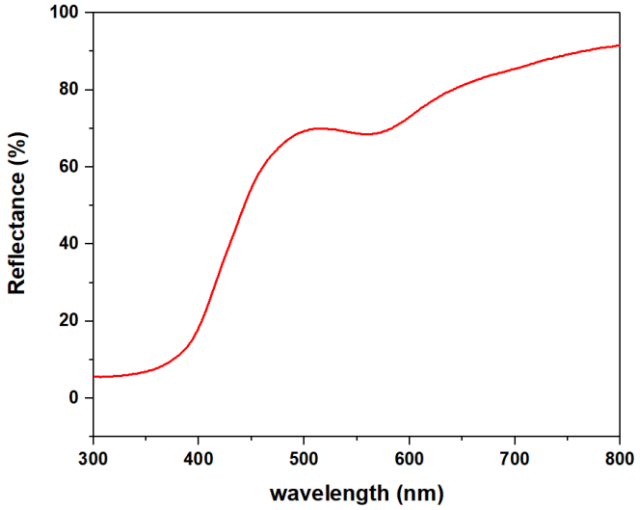

Figure 4. Reflectance data of the synthesized $MnWO_4$ sample via UV-DRS.

The band gap (E_g) of the synthesized $MnWO_4$ was calculated through the extrapolation of the Tauc plot derived from the Kubelka–Munk function. This involved extending the linear portion of the plot to the x-axis where $[F(R)h\nu]^n$ equals zero. Here, F(R) denotes the Kubelka–Munk function or remission function, h stands for Planck's constant (J·s), and ν represents the frequency of the photon (s^{-1}). For the direct band gap, n = 2, and for the indirect band gap, n = 1/2. $MnWO_4$ sample

exhibited [39], [40] both an indirect band gap of 1.72 and 2.76 eV and a direct band gap of 3.18 eV (see Figure 5 and Figure 6).

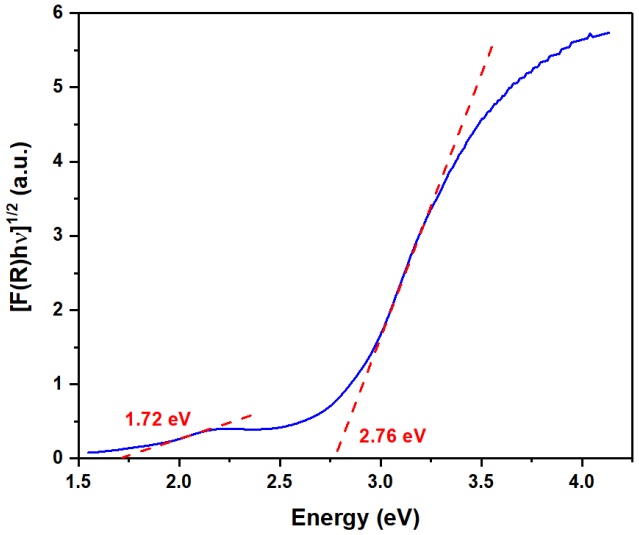

Figure 5. $[F(R)hu]^{1/2}$ versus energy plot via UV-DRS showing the indirect band gap of the synthesized $MnWO_4$.

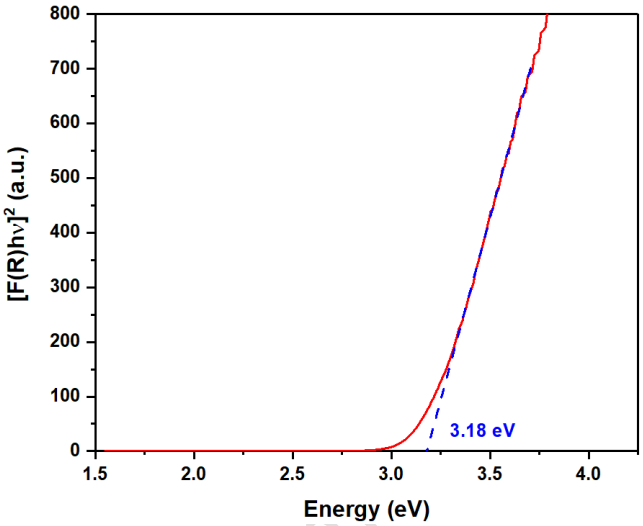

Figure 6. $[F(R)hu]^2$ versus energy plot via UV-DRS showing the direct band gap of the synthesized $MnWO_4$ sample.

The direct band gap of 3.18 eV for $MnWO_4$ positions it as a competitive photocatalyst compared to TiO_2 (~3.2 eV) [41] and ZnO (~3.37 eV) [42]. However, its band gap is slightly larger than that of g-C_3N_4 (~2.7 eV) [43] and $BiVO_4$ (~2.4 eV) [44], which are known for their superior visible-light absorption. To enhance the photocatalytic performance of $MnWO_4$, future studies could explore doping with transition metals or non-metals to reduce the band gap and improve visible-light absorption, as well as forming heterojunctions with other semiconductors to enhance charge separation.

The photocatalytic activity of $MnWO_4$ was evaluated by using the catalyst in an acidic methyl red dye solution. In the UV-Vis analysis, the absorption peak at 518 nm was attributed to methyl red. Following the addition of 200 mg of $MnWO_4$, the solution was left in the dark for 30 minutes to establish a state of adsorption balance. After this adsorption period, UV-C lamps were switched on, and air bubbles were introduced into the reaction vessel. UV spectroscopy measurements were taken at 15-minute intervals, starting from the 0th minute, until the total photocatalytic reaction time reached 180 minutes. Figure 7 presents the UV spectra of the methyl red solution during the photocatalytic reaction, recorded between 0 and 180 minutes.

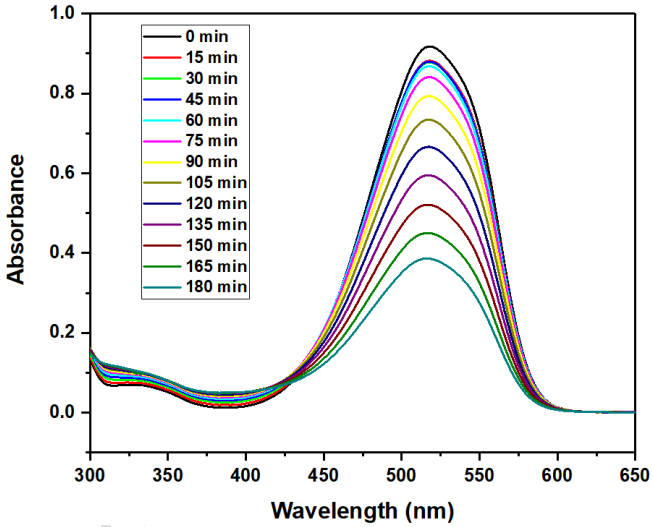

Figure 7. UV-Vis spectra of methyl red solution during photocatalytic breakdown by $MnWO_4$ during a period of 180 minutes. Spectra were recorded at 15-minute intervals, starting from the 0th minute immediately after the adsorption equilibrium was reached, showing the change in absorption at 518 nm as the photocatalytic reaction progressed.

The UV spectra shown in Figure 7 reveal a gradual decrease in the absorbance at 518 nm. This reduction in absorbance indicates the successful degradation of Methyl Red dye over the course of the photocatalytic reaction.

$$Degradation\ Efficiency = 100\frac{(C_0 - C_t)}{C_0} \quad (1)$$

The degradation efficiency of the photocatalytic reaction is calculated according to the equation (1) where C_t and C_0 represent the absorbance values of the methyl red solution at time t and at 0 minutes, respectively, as measured by a UV–Vis spectrometer and presented as a removal efficiency plot in Figure 8.

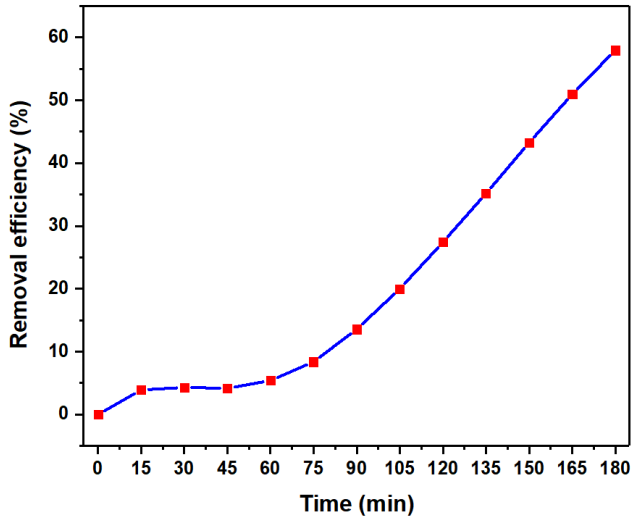

Figure 8. Removal efficiency of $MnWO_4$ on the photodegradation of Methyl Red dye

As shown in Figure 8, the photocatalytic activity initially increased slowly during the first 15 minutes. From 15 to 45 minutes, the removal efficiency remained relatively constant at approximately 5%. In the latter phase of the photocatalytic reaction, the removal efficiency increased rapidly, reaching nearly 60% by the end of the 180-minute reaction.

4 Conclusion

In this study, manganese tungstate ($MnWO_4$) was effectively produced through a simple coprecipitation method and evaluated for its photocatalytic performance in degradating methyl red. The characterization findings confirmed the successful formation of $MnWO_4$ with high crystallinity and suitable optical properties for UV-C light absorption. SEM analysis revealed that the $MnWO_4$ particles exhibited a needle-like morphology with high aspect ratios, which likely contributed to their enhanced photocatalytic activity. The photocatalytic experiments demonstrated that $MnWO_4$ effectively degraded methyl red under UV-C irradiation, with a degradation efficiency of nearly 60% after 180 minutes. This research offers significant understanding and perspectives on the photocatalytic properties of $MnWO_4$ and its potential application in environmental remediation, particularly for the treatment of dye-contaminated wastewater.

5 Acknowledgment

6 Author contribution statements

Within the framework of this research, Author 1 contributed to the conceptualization of the idea, experimental design, procurement of materials, and evaluation of the results. Meanwhile, Author 2 played a role in conducting the literature review, analyzing the findings, and reviewing the manuscript for linguistic accuracy and content quality.

7 Ethics committee approval and conflict of interest statement

There is no need to obtain permission from the ethics committee for the article prepared.

There is no conflict of interest with any person / institution in the article prepared.

8 References

[1] Mofijur M, Hasan MM, Ahmed SF, Djavanroodi F, Fattah IMR, Silitonga AS, Kalam MA, Zhou JL, Khan TMY. ‘‘Advances in identifying and managing emerging contaminants in aquatic ecosystems: Analytical approaches, toxicity assessment, transformation pathways, environmental fate, and remediation strategies’’. *Environmental Pollution,* 341, 122889-122921, 2024

[2] Goswami D, Mukherjee J, Mondal C, Bhunia B. ‘‘Bioremediation of azo dye: A review on strategies, toxicity assessment, mechanisms, bottlenecks and prospects’’. *Science of The Total Environment*, 954, 176426-176445, 2024.

[3] Dutta S, Adhikary S, Bhattacharya S, Roy D, Chatterjee S, Chakraborty A, Banerjee D, Ganguly A, Nanda S, Rajak P. ‘‘Contamination of textile dyes in aquatic environment: Adverse impacts on aquatic ecosystem and human health, and its management using bioremediation’’. *Journal of Environmental Management*, 353, 120103-120125, 2024.

[4] Sahu A, Poler JC. ‘‘Removal and degradation of dyes from textile industry wastewater: Benchmarking recent advancements, toxicity assessment and cost analysis of treatment processes’’. *Journal of Environmental Chemical Engineering*, 12(5), 113754-113786, 2024.

[5] Khandelwal D, Rana I, Mishra V, Ranjan KR, Singh P. ‘‘Unveiling the impact of dyes on aquatic ecosystems through zebrafish – A comprehensive review’’. *Environmental Research*, 261, 119684-119699, 2024.

[6] Kayhan M, Aksoy M, Kayhan E. ‘‘A Facile Synthesis of Photocatalytic Fe(OH)3 Nanoparticles for Degradation of Phenol’’. *ChemistrySelect*, 9(23), e202401367-202401373, 2024.

[7] Kütük N, Çetinkaya S. “Green synthesis of copper oxide nanoparticles using black, green and tarragon tea and investigation of their photocatalytic activity for methylene blue”. *Pamukkale University Journal of Engineering Sciences*, 28(7), 954-962, 2022.

[8] Sma-Air S, Ritchie RJ. ‘‘Methyl red dye decolourization by the photosynthetic bacteria, Rhodopseudomonas palustris and Afifella marina’’. *International Biodeterioration & Biodegradation*, 196, 105915-105924, 2025.

[9] Sargazi S, Ghaneian MT, Rahmani M, Ebrahimi AA. “Application of cloud point extraction coupled with derivative spectrophotometry to remove binary mixture of Cresol Red and Methyl Orange dyes from aqueous solutions: Box–behnken design optimization.” *Heliyon*, 10(21), e39628-39645, 2024.

[10] Riaz U, Farooq A, Alam J. “Microwave-assisted rapid degradation of Methyl red dye using Polyfuran/Polythiophene and its Co-oligomers as catalysts.” *Spectrochimica Acta Part A: Molecular and Biomolecular Spectroscopy*, 302, 123106-123114, 2023.

[11] Sharma S, Sharma S, Sharma KP. “Identification of a sensitive index during fish bioassay of an azo dye methyl

red (untreated and treated)". *Journal of Environmental Biology*, 27(3), 551–555, 2006.

[12] Sharma S, Sharma S, Pathak S, Sharma KP. "Toxicity of the Azo Dye Methyl Red to the Organisms in Microcosms, with Special Reference to the Guppy (Poecilia reticulata Peters)". *Bulletin of Environmental Contamination and Toxicology*, 70(4), 0753–0760, 2003.

[13] Sharma S, Sharma S, Upreti N, Sharma KP. "Monitoring toxicity of an azo dye methyl red and a heavy metal Cu, using plant and animal bioassays". *Toxicology and Environmental Chemistry*, 91(1), 109–120, 2009.

[14] Sievers M. - 4.13, *Advanced Oxidation Processes. in P. Wilderer, ed., Treatise on Water Science*. Oxford: Elsevier, 377–408, 2011

[15] Ghangrekar MM. *Advanced Oxidation Processes. in M.M. Ghangrekar, ed., Wastewater to Water: Principles, Technologies and Engineering Design.* Singapore: Springer Nature Singapore, 733–794, 2022.

[16] Bopape DA, Ntsendwana B, Mabasa FD. "Photocatalysis as a pre-discharge treatment to improve the effect of textile dyes on human health: A critical review". *Heliyon,* 10(20), e39316-39347 2024.

[17] Lanjwani MF, Tuzen M, Khuhawar MY, Saleh TA. "Trends in photocatalytic degradation of organic dye pollutants using nanoparticles: A review". *Inorganic Chemistry Communications*, 159, 111613- 111630, 2024.

[18] Zailan SN, Mahmed N, Bouaissi A, Mubarokah ZR, Norizan MN, Mohamad IS, Yudasari N, Shirajuddin SSM. "Adsorption efficiency and photocatalytic activity of silver sulphide-activated carbon (Ag2S-AC) composites". *Inorganic Chemistry Communications*, 171, 113633-113646, 2025.

[19] Zheng X, Shao Z, Lin J, Gao Q, Ma Z, Song Y, Chen Z, Shi X, Li J, Liu W, Tian X, Liu Y. "Recent advances of CuSbS2 and CuPbSbS3 as photocatalyst in the application of photocatalytic hydrogen evolution and degradation". *Chinese Chemical Letters*, 36, 110533-110548, 2024.

[20] Krishnapuram P, Choudhary J, Kagola UK, Jakka SK. *Photocatalytic and sensing properties of rare-earth doped tungstate upconverting host materials. in V.B. Pawade, S.J. Dhoble, K.N. Shinde, and H.C. Swart, eds., Upconversion Nanocrystals for Sustainable Technology.* Woodhead Publishing, 179–204, 2025.

[21] Abubakar HL, Tijani JO, Abdulkareem AS, Egbosiuba TC, Abdullahi M, Mustapha S, Ajiboye EA. "Effective removal of malachite green from local dyeing wastewater using zinc-tungstate based materials". *Heliyon*, 9(9), e19167-19193, 2023.

[22] Wu H, Peng J, Sun H, Ruan Q, Dong H, Jin Y, Sun Z, Hu Y. "Surface activation of calcium tungstate by europium doping for improving photocatalytic performance: Towards lanthanide site photocatalysis". *Chemical Engineering Journal*, 432, 134339-134349, 2022.

[23] Wei J, Chen Z, Tong Z. "Engineering Z-scheme silver oxide/bismuth tungstate heterostructure incorporated reduced graphene oxide with superior visible-light photocatalytic activity". *Journal of Colloid and Interface Science*, 596, 22–33, 2021.

[24] Wang J, Tang L, Zeng G, Zhou Y, Deng Y, Fan C, Gong J, Liu Y. "Effect of bismuth tungstate with different hierarchical architectures on photocatalytic degradation of norfloxacin under visible light". *Transactions of Nonferrous Metals Society of China*, 27(8), 1794–1803, 2017.

[25] Ahmed AI, Kospa DA, Gamal S, Samra SE, Salah AA, El-Hakam SA, Awad Ibrahim A. "Fast and simple fabrication of reduced graphene oxide-zinc tungstate nanocomposite with enhanced photoresponse properties as a highly efficient indirect sunlight driven photocatalyst and antibacterial agent". *Journal of Photochemistry and Photobiology A: Chemistry*, 429, 13907-13919, 2022.

[26] Rao L, Xu J, Ao Y, Wang P. "Photocatalytic degradation of methyl orange over bismuth tungstate under visible light". *Applied Surface Science*, 315, 191–196. 2014.

[27] Husain M, Rahman N, Azzouz-Rached A, Sfina N, Asad M, Hussain A, Ahmad R, Hamza RD, Humayun Q, Samreen A, Belhachi S, Uzair M, Abualnaja KM, Alosaimi G. "Investigating structural, optoelectronic, and mechanical properties of novel Tungsten-based oxides double-perovskites compounds Sr2XWO6 (X = Mn, Fe): A DFT approach". *Optik*, 315, 172045-172055, 2024.

[28] Harichandran G, Divya P, Radha S, Yesuraj J. "Facile and controllable CTAB-assisted sonochemical synthesis of one-dimensional MnWO4 nanorods for supercapacitor application". *Journal of Molecular Structure*, 1199, 126931-126941 , 2020.

[29] Trung DD, Cuong ND, Trung KQ, Nguyen TD, Van Toan N, Hung CM, Hieu NV. "Controlled synthesis of manganese tungstate nanorods for highly selective NH3 gas sensor". *Journal of Alloys and Compounds*, 735, 787–794, 2018.

[30] Jiang YN, Liu BD, Yang WJ, Yang B, Liu XY, Zhang XL, Mohsin MA, Jiang X. "New strategy for the in situ synthesis of single-crystalline MnWO4/TiO2 photocatalysts for efficient and cyclic photodegradation of organic pollutants". *CrystEngComm*, 18(10), 1832–1841, 2016.

[31] Zhu S, Ho SH, Jin C, Duan X, Wang S. "Nanostructured manganese oxides: natural/artificial formation and their induced catalysis for wastewater remediation". *Environmental Science: Nano*, 7(2), 68–396, 2020.

[32] Islam MA, Morton DW, Johnson BB, Mainali B, Angove MJ. "Manganese oxides and their application to metal ion and contaminant removal from wastewater". *Journal of Water Process Engineering*, 26, 264–280. 2018.

[33] Ishfaq A, Shahid M, Nawaz M, Ibrar D, Hussain S, Shahzad T, Mahmood F, Rais A, Gul S, Gaafar AZ, Hodhod MS, Khan S. "Remediation of wastewater by biosynthesized manganese oxide nanoparticles and its effects on development of wheat seedlings". *Frontiers in Plant Science*, 14, 1263813-1263828, 2023.

[34] Pirhashemi M, Habibi-Yangjeh A. "Fabrication of novel ZnO/MnWO4 nanocomposites with p-n heterojunction: Visible-light-induced photocatalysts with substantially improved activity and durability". *Journal of Materials Science & Technology*, 34(10), 1891–1901, 2018.

[35] Zheng M, Zhang H, Gong X, Xu R, Xiao Y, Dong H, Liu X, Liu Y. "A simple additive-free approach for the synthesis of uniform manganese monoxide nanorods with large

specific surface area". *Nanoscale Research Letters*, 8(1), 166-173, 2013.

[36] Muthamizh S, Suresh R, Giribabu K, Manigandan R, Praveen Kumar S, Munusamy S, Narayanan V. "MnWO4 nanocapsules: Synthesis, characterization and its electrochemical sensing property". *Journal of Alloys and Compounds*, 619, 601–609, 2015.

[37] Nogami A, Suzuki T, Katsufuji T. "Second Harmonic Generation from Multiferroic MnWO4". *Journal of the Physical Society of Japan*, 77(11), 115001-115003, 2008.

[38] Van Hanh P, Hoang LH, Hai PV, Minh NV, Chen XB, Yang IS. "Crystal quality and optical property of MnWO4 nanoparticles synthesized by microwave-assisted method". J*ournal of Physics and Chemistry of Solids*, 74(3), 426–430, 2013.

[39] Chakraborty AK, Ganguli S, Kebede MA. "Photocatalytic degradation of 2-propanol and phenol using Au-loaded MnWO4 nanorod under visible light irradiation". *Journal of Cluster Science*, 23(2), 437–448, 2012.

[40] Almeida MAP, Cavalcante LS, Varela JA, Li MS, Longo E. "Effect of different surfactants on the shape, growth, and photoluminescence behavior of MnWO4 crystals synthesized by the microwave-hydrothermal method". *Advances in Powder Technology*, 23(1), 124–128, 2012.

[41] Kayhan E. "Graphene: Synthesis, Characterization, Properties and Functional Behavior as Catalyst Support and Gas Sensor". Ph.D. Thesis, Technische Universität Darmstadt, Darmstadt, Germany, 2013.

[42] Jafarova VN, Orudzhev GS. "Structural and electronic properties of ZnO: A first-principles density-functional theory study within LDA(GGA) and LDA(GGA)+U methods". *Solid State Communications,* 325, 114166, 2021.

[43] Bilal M, Wang L, Ur Rehman Z, Zheng K, Hou J, Butt FK, Hussain A, Ahmad J, Ullah S, Jrar JA, Ali S, Wang X. "Hydrogen production using g-C3N4 based photocatalysts: A review". *International Journal of Hydrogen Energy,* 96, 456-473, 2024.

[44] Kamble GS, Natarajan TS, Patil SS, Thomas M, Chougale RK, Sanadi PD, Siddharth US, Ling YC. "$BiVO_4$ As a Sustainable and Emerging Photocatalyst: Synthesis Methodologies, Engineering Properties, and Its Volatile Organic Compounds Degradation Efficiency". *Nanomaterials (Basel)*, 13(9), 1528, 2023.